Supporting Information

High-throughput screening of small, eco-friendly, molecular crystals for sustainable piezoelectric materials

Shubham Vishnoi[1], Geetu Kumari[1], Robert Guest[1], Pierre-Andre Cazade[2], Sarah Guerin[1, 3*]

[1]*Department of Chemical Sciences, Bernal Institute, University of Limerick, V94 T9PX, Ireland*

[2]*Department of Physics, Bernal Institute, University of Limerick, V94 T9PX, Ireland*

[3]*SSPC, The Science Foundation Ireland Research Centre for Pharmaceuticals, University of Limerick, V94 T9PX, Ireland*

Table of Contents

Supplementary Notes

List of Figure

List of Tables

Supplementary Notes

S1. Flagging Criteria in CrystalDFT High-throughput Workflow: *In the high-throughput workflow described in this study, a set of criteria is used to flag crystal structures for further examination when predicted properties fall outside predefined ranges. These criteria help ensure that the workflow focuses on stable, meaningful results and filters out anomalous outputs caused by errors or instabilities. Below is a detailed explanation of the flagging process and its implications:*

1. Abnormal Dielectric Constant: *Crystals with a* ***predicted dielectric constant*** *(ε) greater than* ***5*** *are flagged. Such values often indicate protonation errors or other inaccuracies in the initial structure or calculations.*

2. Mechanical Instability: *Crystals with a predicted elastic constant below* ***1 GPa*** *are flagged. This suggests structural instability, as such low stiffness values are inconsistent with mechanically sound materials.*

3. Numerical Instabilities: *Crystals with* ***high condition numbers*** *(CN > 100) are flagged. A high condition number implies numerical instability in the calculations, which can lead to unreliable results.*

4. Negative Eigenvalues: *Crystals with* ***negative eigenvalues*** *in the calculated tensors are flagged. This typically indicates an issue with the stability of the structure or calculation errors[1].*

S2. Workflow Overview: *The automated workflow integrates these criteria into its decision-making process. Structures that meet the above conditions are automatically excluded from further high-throughput screening and marked with flagged notation. *However, the condition number flag is not applied stringently across all analyses and is only used for specific figures, as noted in the captions for those particular figures. All other flags are applied rigorously throughout the study. This could prevent errors from propagating through the dataset and allows future studies and computational resources to focus on promising candidates.*

CrystalDFT Workflow Script and Database: The workflow was constructed using Python-based libraries, which facilitates the pre-selection, input file preparation (Atomic Simulation Environment, ASE[2]), formatting, optimization (via DFT - VASP[3]), electromechanical property prediction of the input crystal structures and output processing (for additional details and access *to scripts, please refer to - https://actuatelab.ie/actuate_tools.html). The CrystalDFT database (**Figure S1 - https://actuatelab.ie/CrystalDFT/index.html**) also includes visualisation of tensors based on calculation outputs, along with several widgets (such as HD Viewer, 3D Visualiser – integrated with JSmol[4], Crystal Card), illustrating key details related to crystal structure (including symmetry and molecular information), predicted tensors, and decision points such as flagging and further analysis. We used MTEX[5] for visualising polarisation in 3D. This rigorous flagging and evaluation process ensures high reliability and efficiency in identifying promising organic piezoelectric materials.*

*Testing and Screening Outcomes: A total of **572 crystal structures** were evaluated in this study. Structures flagged for any of the above criteria were excluded from the final analysis. After applying these filters, 22 crystals were identified that exhibited double-digit piezoelectric coefficients (measured in pC/N), meeting the stringent stability and performance thresholds defined in the workflow.*

Figure

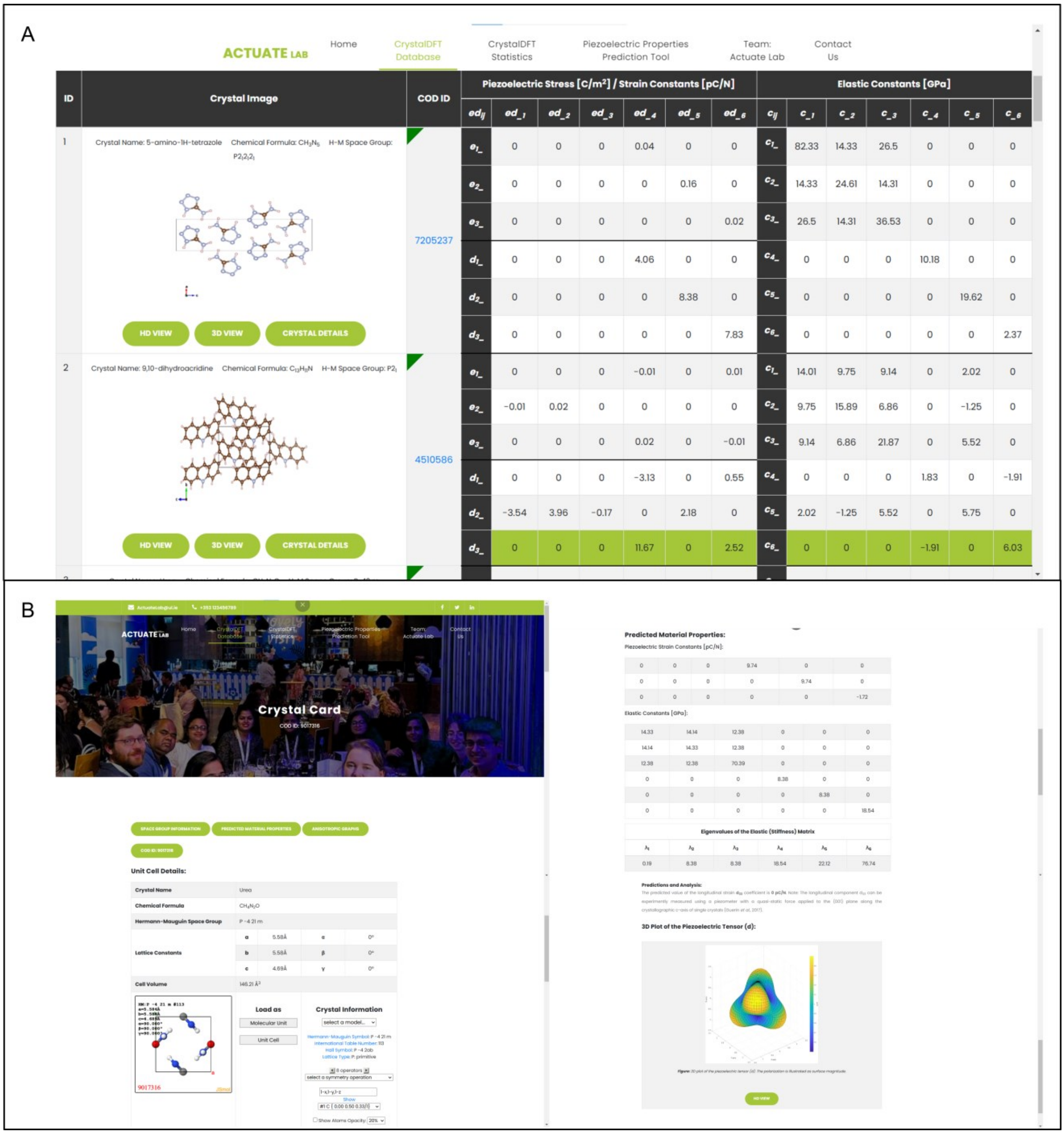

Figure S1. The CrystalDFT database provides a comprehensive set of tools for visualising and analysing our DFT-predicted piezoelectric tensors and crystal data along with the links to the relevant resources. **A.** It includes advanced visualisation features for tensors derived from calculation outputs, along with interactive widgets such as the HD Viewer, 3D Visualiser, and **B.** Crystal Card. These tools offer detailed insights into crystal structures, including symmetry and molecular information, as well as predicted tensors and key decision points, such as flagging details and other derived properties. Database Website Link: https://actuatelab.ie/CrystalDFT/index.html.

Tables

Table S1A. Reported maximum piezoelectric response in pC/N for a variety of piezoelectric materials, as plotted in **Figure 1** in the main text.

Material	Piezoelectric Strain Coefficient (pC/N)	Category
Collagen[6]	12	Bioorganics
γ-Glycine[7]	9.9	Bioorganics
L-Alanine[8]	6	Bioorganics
Hydroxy-L-Proline (Single Crystal)[9]	25	Bioorganics
Hydroxy-L-Proline (Film)[10]	1.5	Bioorganics
L-Threonine (Film)[10]	0.2	Bioorganics
Hydroxyapatite (Poled Ceramic)[11]	2	Bioorganics
M13 Bacteriophage Virus[12]	10	Bioorganics
Bone[13]	0.2	Bioorganics
Wood[14]	0.1	Bioorganics
Dry Tendon[15]	2	Bioorganics
Wool[16]	0.1	Bioorganics
Horn[16]	1.8	Bioorganics
Starch[16]	2	Bioorganics
Glycine Nanofibers[17]	12.5	Bioorganics
Spar[18]	0.02	Bioorganics
Lysozyme (Film)[19]	6.5	Bioorganics
Chitin Nanofiber[20]	2	Bioorganics
Gelatine Nanofiber[21]	20	Bioorganics
Di-Phenylalanine (FF) Peptide Nanotubes[22]	60	Bioorganics
Chitosan[23]	6	Bioorganics
CNF[23]	8	Bioorganics
Eggshell Membrane[24]	18.3	Bioorganics
Silk[25]	56.2	Bioorganics
Di-Phenylalanine (FF) Microribbon[26]	40	Bioorganics
L-Asparagine[7]	13	Bioorganics
L-Leucine[7]	20	Bioorganics
L-Histidine[7]	18	Bioorganics
L-Methionine[7]	15	Bioorganics
L-Aspartate[7]	13	Bioorganics
L-Isoleucine[7]	25	Bioorganics
L-Cysteine[7]	11	Bioorganics
DL-Alanine[27]	4	Bioorganics
Poly(Î³-benzyl-l-glutamate)(PBLG)[28]	25	Biopolymers
Polymethyl-L-Glutamate (PMG)[16]	2	Biopolymers
Poly-Lactic-Acid (PLA)[16]	10	Biopolymers
Porous Polypropylene (p-PP)[29]	450	Polymers
Poly-b-Hydroxybutyrate[16]	1.3	Polymers
PVDF (Poled)[30]	32	Polymers
Propylene Oxide[16]	0.1	Polymers
P(VDF-TRFE)[31]	40	Polymers

Lithium Niobate[32]	42	Inorganics
Quartz[33]	2.3	Inorganics
BiB_3O_6[34]	40	Inorganics
$BiFeO_3$[35]	18	Inorganics
$BaTiO_3$	90	Inorganics
Al_3AsO_7[36]	9	Inorganics
Al_3PO_7[36]	3.4	Inorganics
Ga_3AsO_7[36]	23.9	Inorganics
$GaPO_7$[36]	8.2	Inorganics
ZnO[37]	9.9	Inorganics
AlN[38]	5.4	Inorganics
Barium Titanate (Single Crystal)[39]	392	Inorganics
Rochelle Salt[40]	345	Inorganics
CBT[41]	8	Inorganics
NBBT95/5[42]	360	Inorganics
Mn-KNN[43]	350	Inorganics
BZT-BCT[44]	637	Inorganics
Lead Zirconium Titanate (PZT)[45]	493	Lead-containing
Barium Titanate (Ceramic)[39]	270	Inorganics
Potassium-Sodium Niobate[46]	490	Inorganics
$GaPBi_3$[47]	146	Inorganics
GeSe[48]	212	Inorganics
SnS[48]	145	Inorganics
SnSe[48]	251	Inorganics
GeS[48]	75	Inorganics
ZnO Nanorods[49]	9.5	Nanostructures
PZT Nanoshell[50]	90	Lead-containing
GaN Nanowires[51]	12.8	Nanostructures
PZT ceramic[52]	407.4	Lead-containing

Table 1B. Summary of the averages and ranges for each category listed in Supplementary Information **Table S1A**, with the median providing an additional measure of central tendency. These values indicate currently observed potential for applications in energy harvesting and sensing, with detailed data in **Table S1A**.

Category	Average (pC/N)	Median (pC/N)	Range	Standard Deviation
Bioorganics	13.11	10	0.02 to 60	15.28
Biopolymers	12.33	10	2 to 25	11.68
Polymers	104.68	32	0.1 to 450	193.87
Inorganics	167.09	75	2.3 to 637	186.10

Lead-containing	330.13	407.4	90 to 493	212.32
Nanostructures	11.15	11.15	9.5 to 12.8	2.33

Table S2. Hermann-Mauguin Space Group Symbols and Corresponding Space Group Numbers. Only structures with space groups 1, 3–9, 16–46, 75–82, 89–122, 143–146, 149–161, 168–174, 177–190, 195–199, 207–220 are allowed (since these space groups lack inversion symmetry).

1	P 1	2	P -1	3	P 2	4	$P\ 2_1$	5	C 2
6	P m	7	P c	8	C m	9	C c	10	P 2/m
11	$P\ 2_1/m$	12	C 2/m	13	P 2/c	14	$P\ 2_1/c$	15	C 2/c
16	P 2 2 2	17	$P\ 2\ 2\ 2_1$	18	$P\ 2_1\ 2_1\ 2$	19	$P\ 2_1\ 2_1\ 2_1$	20	$C\ 2\ 2\ 2_1$
21	C 2 2 2	22	F 2 2 2	23	I 2 2 2	24	$I\ 2_1\ 2_1\ 2_1$	25	P m m 2
26	$P\ m\ c\ 2_1$	27	P c c 2	28	P m a 2	29	$P\ c\ a\ 2_1$	30	P n c 2
31	$P\ m\ n\ 2_1$	32	P b a 2	33	$P\ n\ a\ 2_1$	34	P n n 2	35	C m m 2
36	$C\ m\ c\ 2_1$	37	C c c 2	38	A m m 2	39	A b m 2	40	A m a 2
41	A b a 2	42	F m m 2	43	F d d 2	44	I m m 2	45	I b a 2
46	I m a 2	47	P m m m	48	P n n n	49	P c c m	50	P b a n
51	P m m a	52	P n n a	53	P m n a	54	P c c a	55	P b a m
56	P c c n	57	P b c m	58	P n n m	59	P m m n	60	P b c n
61	P b c a	62	P n m a	63	C m c m	64	C m c a	65	C m m m
66	C c c m	67	C m m a	68	C c c a	69	F m m m	70	F d d d
71	I m m m	72	I b a m	73	I b c a	74	I m m a	75	P 4
76	$P\ 4_1$	77	$P\ 4_2$	78	$P\ 4_3$	79	I 4	80	$I\ 4_1$
81	P -4	82	I -4	83	P 4/m	84	$P\ 4_2/m$	85	P 4/n

86	P 4_2/n	87	I 4/m	88	I 4_1/a	89	P 4 2 2	90	P 4 2_1 2
91	P 4_1 2 2	92	P 4_1 2_1 2	93	P 4_2 2 2	94	P 4_2 2_1 2	95	P 4_3 2 2
96	P 4_3 2_1 2	97	I 4 2 2	98	I 4_1 2 2	99	P 4 m m	100	P 4 b m
101	P 4_2 c m	102	P 4_2 n m	103	P 4 c c	104	P 4 n c	105	P 4_2 m c
106	P 4_2 b c	107	I 4 m m	108	I 4 c m	109	I 4_1 m d	110	I 4_1 c d
111	P -4 2 m	112	P -4 2 c	113	P -4 2_1 m	114	P -4 2_1 c	115	P -4 m 2
116	P -4 c 2	117	P -4 b 2	118	P -4 n 2	119	I -4 m 2	120	I -4 c 2
121	I -4 2 m	122	I -4 2 d	123	P 4/m m m	124	P 4/m c c	125	P 4/n b m
126	P 4/n n c	127	P 4/m b m	128	P 4/m n c	129	P 4/n m m	130	P 4/n c c
131	P 4_2/m m c	132	P 4_2/m c m	133	P 4_2/n b c	134	P 4_2/n n m	135	P 4_2/m b c
136	P 4_2/m n m	137	P 4_2/n m c	138	P 4_2/n c m	139	I 4/m m m	140	I 4/m c m
141	I 4_1/a m d	142	I 4_1/a c d	143	P 3	144	P 3_1	145	P 3_2
146	R 3	147	P -3	148	R -3	149	P 3 1 2	150	P 3 2 1
151	P 3_1 1 2	152	P 3_1 2 1	153	P 3_2 1 2	154	P 3_2 2 1	155	R 3 2
156	P 3 m 1	157	P 3 1 m	158	P 3 c 1	159	P 3 1 c	160	R 3 m
161	R 3 c	162	P -3 1 m	163	P -3 1 c	164	P -3 m 1	165	P -3 c 1
166	R -3 m	167	R -3 c	168	P 6	169	P 6_1	170	P 6_5
171	P 6_2	172	P 6_4	173	P 6_3	174	P -6	175	P 6/m
176	P 6_3/m	177	P 6 2 2	178	P 6_1 2 2	179	P 6_5 2 2	180	P 6_2 2 2
181	P 6_4 2 2	182	P 6_3 2 2	183	P 6 m m	184	P 6 c c	185	P 6_3 c m
186	P 6_3 m c	187	P -6 m 2	188	P -6 c 2	189	P -6 2 m	190	P -6 2 c
191	P 6/m m m	192	P 6/m c c	193	P 6_3/m c m	194	P 6_3/m m c	195	P 2 3

196	F 2 3	197	I 2 3	198	P 2_1 3	199	I 2_1 3	200	P m -3
201	P n -3	202	F m -3	203	F d -3	204	I m -3	205	P a -3
206	I a -3	207	P 4 3 2	208	P 4_2 3 2	209	F 4 3 2	210	F 4_1 3 2
211	I 4 3 2	212	P 4_3 3 2	213	P 4_1 3 2	214	I 4_1 3 2	215	P -4 3 m
216	F -4 3 m	217	I -4 3 m	218	P -4 3 n	219	F -4 3 c	220	I -4 3 d
221	P m -3 m	222	P n -3 n	223	P m -3 n	224	P n -3 m	225	F m -3 m
226	F m -3 c	227	F d -3 m	228	F d -3 c	229	I m -3 m	230	I a -3 d

Table S3. Calculated piezoelectric strain coefficients for a range of well-known inorganic crystals, including zinc oxide, aluminium nitride, α-quartz, and additional materials for comprehensive comparison (Citations).

Crystal Name		Piezoelectric strain coefficients (pC/N)					
		d_{11}	d_{22}	d_{15}	d_{31}	d_{32}	d_{33}
Zinc Oxide (ZnO)	Predictions			*12.2*	*6*		*11.8*
	Experiments			*8.3*	*5.1*		*12.3*
Aluminium Nitride (AlN) (1605321)	Predictions			*3.7*	*1.7*		*5.6*
	Experiments			*4.08*	*2.65*		*5.53*
α-quartz - Silicon Dioxide (SiO_2)	Predictions	*2.2*		*0.76*			
	Experiments	*2.3*		*0.73*			
$BaTiO_3$	Predictions			*2.5*	*19.2*		*67.2*
	Experiments			*392*	*34.5*		*85.6* *90*
$KNbO_3$ (1594511)	Predictions				*16.7*	*12.7*	*21.1*
	Experiments				*22.3*	*15.5*	*29.6*
$LiTaO_3$	Predictions		*11*	*29.5*	*2.48*		*7.59*

(1594518)	Experiments		*8.5*	*26*	*3*		*9.2*
$LiNbO_3$	Predictions						*7.67*
	Experiments						*7.9*
Graphene oxide	1568395	**Has been studied for its piezoelectric properties both computationally[53] and experimentally[54, 55]**					
Cristobalite	9015590	**Related report available[56]**					

Table S4. Summary of organic single crystal systems used for the comparison of calculated and experimental piezoelectric constants. For comparison purposes, we merged this data with the data from **Table S3**, which includes several well-known inorganic crystals and materials tested in-house, to provide a broader context against experimental measurements, as there are still very few small organic materials characterized for their piezoelectric properties. The table details the crystal name, reported experimental values, and corresponding calculated piezoelectric coefficients for each system.

Crystal Name	**COD ID/CSD ID**	**Experimental Piezoelectric strain coefficients** *(pC/N)*						**DFT-predicted Piezoelectric strain coefficients** *(pC/N)*					
		d_{11}	d_{14}	d_{15}	d_{16}	d_{31}	d_{33}	d_{11}	d_{14}	d_{15}	d_{16}	d_{31}	d_{33}
γ-Glycine	7128793			**5.33**			*11.33*			*5.15*			*10.72*
L-histidine	2108877/2108883						*18 (d_{24})*						*18.49/20.68 (d_{24})*
L-Aspartate	2015971				*13*						*13.2*		
DL-Alanine							*10.8*						*10.3*
DL-Tyrosine							*8.64*						*8.4*
l-lactic acid			**10**						*11.72*				
β-Glycine	4505645				**178**						**50.66**		**12.07**

Cellulose[57]	4114383						5.85						11.91
L-Asparagine	2215317						13 (d_{16})						11.02 (d_{16})
L-ornithine Hydrochloride		Reported - NLO[58]											
DL-malic acid	5000188	Reported with Piezoelectric Response[59]											
Malic Acid		Derivatives Reported with Piezoelectric Responses[60]											
Tartaric Acid and its derivatives	2008148	Derivatives Reported with Piezoelectric Responses[61]						Max Predicted Strain: -21.47					
L-Threonine[10]	5000016	0.1 (d_{33})						0.14 (d_{33})					
N-methylurea	7209247	Previously has been gone under related piezoelectric study[62]											
Methylpiperazine	2105466	Has been reported as in chiral hybrid metal halides R/SMPCdCl4 (R/SMP = R-/S-2-methylpiperazine)[63]						-10.58 (d_{14})					
5-aminotetrazolium dinitramide	7000350	Derivatives reported as energetic materials[64]											
p-nitrobenzaldehyde	2005110	Reported for Electrical, Optical and Mechanical properties[65]											

Table S5. Summary of amino acid single crystal systems used for the comparison of calculated and experimental piezoelectric constants. Add – COD ID, References.

Amino Acid Crystal Name	CrystalDFT Predictions (pC/N)	Experimental/Simulation Data (Literature) (pC/N)
L-Alanine	5.7	6.3
L-Arginine	6.76	6.5

L-Asparagine	11.02	13
L-Aspartate	13.2	13
L-Cysteine	10.19	11.4
γ-Glycine	10.72	11.33
L-histidine	18.49	18
L-Leucine	13.33	8.6
L-Methionine	17.18	15
L-Threonine	13.46	4.9
L-Threonine	0.1	0.14
DL-Alanine	10.3	10.8
DL-Tyrosine	8.4	8.64

Table S6. Summary of functional group representation within the CrystalDFT database, showing total occurrences of each functional group and their respective percentage within the dataset. The table also includes the count of each functional group within the HTS unflagged subset of CrystalDFT database and the percentage representation of each within this subset. Notably, we used RDKit[66] to analyse functional groups, following the generation of SMILES notation for each crystal molecular entity using Open Babel[67]. Crystals for which RDKit analysis failed were excluded from the analysis. This subset is refined to exclude crystals with high dielectric constants, negative stiffness or high condition numbers, ensuring a focus on functional groups that contribute to stable and reliable piezoelectric properties.

Functional Group	Full CrystalDFT Dataset		HTS Unflagged Subset	
	Total Count	Percentage (%)	Total Count	Percentage (%)
Hydroxyl	216	49	145	57.8
Aldehyde	257	58.3	151	60.2
Ketone	148	33.6	102	40.6
Carboxylic Acid	140	31.7	90	35.9
Amino	263	59.6	151	60.2
Amide	128	29	79	31.5
Ester	140	31.7	90	35.9
Nitrile	26	5.9	15	6

Alkane	368	83.4	220	87.6
Alkene	73	16.6	37	14.7
Alkyne	9	2	5	2
Ether	85	19.3	70	27.9
Cycloalkane	17	3.9	10	4
Aromatic Ring	148	33.6	90	35.9
Pyridine	14	3.2	7	2.8

References

1. Yalameha, S.; Nourbakhsh, Z.; Vashaee, D., ElATools: A tool for analyzing anisotropic elastic properties of the 2D and 3D materials. *Computer Physics Communications* **2022,** *271*, 108195.

2. Hjorth Larsen, A.; Jørgen Mortensen, J.; Blomqvist, J.*, et al.*, The atomic simulation environment—a Python library for working with atoms. *Journal of Physics: Condensed Matter* **2017,** *29* (27), 273002.

3. Hafner, J., Materials simulations using VASP—a quantum perspective to materials science. *Computer Physics Communications* **2007,** *177* (1), 6-13.

4. Hanson, R. M.; Prilusky, J.; Renjian, Z.*, et al.*, JSmol and the next-generation web-based representation of 3D molecular structure as applied to proteopedia. *Israel Journal of Chemistry* **2013,** *53* (3-4), 207-216.

5. Mainprice, D.; Bachmann, F.; Hielscher, R.*, et al.*, Calculating anisotropic piezoelectric properties from texture data using the MTEX open source package. *Geological Society, London, Special Publications* **2015,** *409* (1), 223-249.

6. Denning, D.; Kilpatrick, J. I.; Fukada, E.*, et al.*, Piezoelectric Tensor of Collagen Fibrils Determined at the Nanoscale. *ACS Biomaterials Science & Engineering* **2017,** *3* (6), 929-935.

7. Guerin, S.; Stapleton, A.; Chovan, D.*, et al.*, Control of piezoelectricity in amino acids by supramolecular packing. *Nature Materials* **2018,** *17* (2), 180-186.

8. Tylczyński, Z.; Sterczyńska, A.; Wiesner, M., Temperature dependences of piezoelectric, elastic and dielectric constants of L-alanine crystal. *J Phys Condens Matter* **2011,** *23* (35), 355901.

9. Guerin, S.; Syed, T. A. M.; Thompson, D., Deconstructing collagen piezoelectricity using alanine-hydroxyproline-glycine building blocks. *Nanoscale* **2018,** *10* (20), 9653-9663.

10. Guerin, S.; Tofail, S. A. M.; Thompson, D., Longitudinal Piezoelectricity in Orthorhombic Amino Acid Crystal Films. *Crystal Growth & Design* **2018,** *18* (9), 4844-4848.

11. Gandhi, A. A.; Wojtas, M.; Lang, S. B.*, et al.*, Piezoelectricity in Poled Hydroxyapatite Ceramics. *Journal of the American Ceramic Society* **2014,** *97* (9), 2867-2872.

12. Lee, B. Y.; Zhang, J.; Zueger, C.*, et al.*, Virus-based piezoelectric energy generation. *Nature Nanotechnology* **2012,** *7* (6), 351-356.

13. Fukada, E.; Yasuda, I., On the Piezoelectric Effect of Bone. *Journal of the Physical Society of Japan* **1957,** *12* (10), 1158-1162.

14. Fukada, E., Piezoelectricity of Wood. *Journal of the Physical Society of Japan* **1955,** *10* (2), 149-154.

15. Fukada, E.; Yasuda, I., Piezoelectric Effects in Collagen. *Japanese Journal of Applied Physics* **1964,** *3* (2), 117.

16. Fukada, E., History and recent progress in piezoelectric polymers. *IEEE Trans Ultrason Ferroelectr Freq Control* **2000,** *47* (6), 1277-90.

17. Isakov, D.; Gomes, E. d. M.; Bdikin, I.*, et al.*, Production of Polar β-Glycine Nanofibers with Enhanced Nonlinear Optical and Piezoelectric Properties. *Crystal Growth & Design* **2011,** *11* (10), 4288-4291.

18. Guerin, S.; Tofail, S. A. M.; Thompson, D., Longitudinal piezoelectricity in natural calcite materials: Preliminary studies. *IEEE Transactions on Dielectrics and Electrical Insulation* **2018,** *25* (3), 803-807.

19. Stapleton, A.; Noor, M. R.; Sweeney, J., *et al.*, The direct piezoelectric effect in the globular protein lysozyme. *Applied Physics Letters* **2017,** *111* (14).

20. Hoque, N. A.; Thakur, P.; Biswas, P., *et al.*, Biowaste crab shell-extracted chitin nanofiber-based superior piezoelectric nanogenerator. *Journal of Materials Chemistry A* **2018,** *6* (28), 13848-13858.

21. Ghosh, S. K.; Adhikary, P.; Jana, S., *et al.*, Electrospun gelatin nanofiber based self-powered bio-e-skin for health care monitoring. *Nano Energy* **2017,** *36*, 166-175.

22. Kholkin, A.; Amdursky, N.; Bdikin, I., *et al.*, Strong Piezoelectricity in Bioinspired Peptide Nanotubes. *ACS Nano* **2010,** *4* (2), 610-614.

23. Hänninen, A.; Sarlin, E.; Lyyra, I., *et al.*, Nanocellulose and chitosan based films as low cost, green piezoelectric materials. *Carbohydrate Polymers* **2018,** *202*, 418-424.

24. Karan, S. K.; Maiti, S.; Paria, S., *et al.*, A new insight towards eggshell membrane as high energy conversion efficient bio-piezoelectric energy harvester. *Materials Today Energy* **2018,** *9*, 114-125.

25. Joseph, J.; Singh, S. G.; Vanjari, S. R. K., Piezoelectric Micromachined Ultrasonic Transducer Using Silk Piezoelectric Thin Film. *IEEE Electron Device Letters* **2018,** *39* (5), 749-752.

26. Safaryan, S.; Slabov, V.; Kopyl, S., *et al.*, Diphenylalanine-Based Microribbons for Piezoelectric Applications via Inkjet Printing. *ACS Applied Materials & Interfaces* **2018,** *10* (12), 10543-10551.

27. Dai, F.; Geng, Q.; Hua, T., *et al.*, Organic biodegradable piezoelectric materials and their potential applications as bioelectronics. *Soft Science* **2023,** *3* (1), N/A-N/A.

28. Farrar, D.; Ren, K.; Cheng, D., *et al.*, Permanent Polarity and Piezoelectricity of Electrospun α-Helical Poly(α-Amino Acid) Fibers. *Advanced Materials* **2011,** *23* (34), 3954-3958.

29. Kodama, H.; Yasuno, Y.; Furukawa, T., *et al.* In *Electromechanical properties and acoustic applications of high sensitivity porous polypropylene electrets*, International Workshop on Smart Materials and Structures and NDT in Aerospace, Conference on NDT in Canada, 2011.

30. Murayama, N.; Nakamura, K.; Obara, H., *et al.*, The strong piezoelectricity in polyvinylidene fluroide (PVDF). *Ultrasonics* **1976,** *14* (1), 15-24.

31. Lovinger, A. J., Ferroelectric Polymers. *Science* **1983,** *220* (4602), 1115-1121.

32. Smith, R. T.; Welsh, F. S., Temperature Dependence of the Elastic, Piezoelectric, and Dielectric Constants of Lithium Tantalate and Lithium Niobate. *Journal of Applied Physics* **1971,** *42* (6), 2219-2230.

33. Bechmann, R., Elastic and Piezoelectric Constants of Alpha-Quartz. *Physical Review* **1958,** *110* (5), 1060-1061.

34. Yu, F.; Lu, Q.; Zhang, S., *et al.*, High-performance, high-temperature piezoelectric BiB3O6 crystals. *Journal of Materials Chemistry C* **2015,** *3* (2), 329-338.

35. Graf, M.; Sepliarsky, M.; Machado, R., *et al.*, Dielectric and piezoelectric properties of BiFeO3 from molecular dynamics simulations. *Solid State Communications* **2015,** *218*, 10-13.

36. Ren, J.; Ma, Z.; He, C., *et al.*, Structure, elastic and piezoelectric properties of A3BO7 (A= Ga, Al; B= P, As) compounds: A DFT study. *Computational Materials Science* **2015,** *106*, 1-4.

37. Kobiakov, I. B., Elastic, piezoelectric and dielectric properties of ZnO and CdS single crystals in a wide range of temperatures. *Solid State Communications* **1980,** *35* (3), 305-310.

38. Zha, X.-H.; Ma, X.; Luo, J.-T., *et al.*, Enhanced piezoelectric response of AlN via alloying of transitional metals, and influence of type and distribution of transition metals. *Nano Energy* **2023,** *111*, 108390.

39. Berlincourt, D.; Jaffe, H., Elastic and Piezoelectric Coefficients of Single-Crystal Barium Titanate. *Physical Review* **1958,** *111* (1), 143-148.

40. Mason, W. P., A Dynamic Measurement of the Elastic, Electric and Piezoelectric Constants of Rochelle Salt. *Physical Review* **1939,** *55* (8), 775-789.

41. Peng, D.; Wang, X.; Xu, C., *et al.*, Bright Upconversion Emission, Increased Tc, Enhanced Ferroelectric and Piezoelectric Properties in r-Doped 4415 Multifunctional Ferroelectric Oxides. *Journal of the American Ceramic Society* **2013,** *96* (1), 184-190.

42. Zheng, L.; Yi, X.; Zhang, S., *et al.*, Complete set of material constants of 0.95(Na0.5Bi0.5)TiO3-0.05BaTiO3 lead-free piezoelectric single crystal and the delineation of extrinsic contributions. *Applied Physics Letters* **2013,** *103* (12).

43. Lin, D.; Zhang, S.; Cai, C., *et al.*, Domain size engineering in 0.5%MnO2-(K0.5Na0.5)NbO3 lead free piezoelectric crystals. *Journal of Applied Physics* **2015,** *117* (7).

44. Praveen, J. P.; Karthik, T.; James, A. R., *et al.*, Effect of poling process on piezoelectric properties of sol–gel derived BZT–BCT ceramics. *Journal of the European Ceramic Society* **2015,** *35* (6), 1785-1798.

45. Guo, Q.; Cao, G. Z.; Shen, I. Y., Measurements of Piezoelectric Coefficient d33 of Lead Zirconate Titanate Thin Films Using a Mini Force Hammer. *Journal of Vibration and Acoustics* **2013,** *135* (1).

46. Wang, X.; Wu, J.; Xiao, D., *et al.*, Giant Piezoelectricity in Potassium–Sodium Niobate Lead-Free Ceramics. *Journal of the American Chemical Society* **2014,** *136* (7), 2905-2910.

47. Tang, G.; Hong, J., Direct tuning of the band gap via electronically-active organic cations and large piezoelectric response in one-dimensional hybrid halides from first-principles. *Journal of Materials Chemistry C* **2018,** *6* (28), 7671-7676.

48. Fei, R.; Li, W.; Li, J., *et al.*, Giant piezoelectricity of monolayer group IV monochalcogenides: SnSe, SnS, GeSe, and GeS. *Applied Physics Letters* **2015,** *107* (17).

49. Scrymgeour, D. A.; Hsu, J. W. P., Correlated Piezoelectric and Electrical Properties in Individual ZnO Nanorods. *Nano Letters* **2008,** *8* (8), 2204-2209.

50. Luo, Y.; Szafraniak, I.; Zakharov, N. D., *et al.*, Nanoshell tubes of ferroelectric lead zirconate titanate and barium titanate. *Applied Physics Letters* **2003,** *83* (3), 440-442.

51. Minary-Jolandan, M.; Bernal, R. A.; Kuljanishvili, I., *et al.*, Individual GaN Nanowires Exhibit Strong Piezoelectricity in 3D. *Nano Letters* **2012,** *12* (2), 970-976.

52. LIU, M.-w.; DONG, W.-j.; TONG, J.-h., *et al.* In *Measurement of longitudinal piezoelectric coefficients (d33) of Pb (Zr0. 50, Ti0. 50) O3 thin films with atomic force microscopy*, Proceedings of the Third International Symposium on Instrumentation Science and Technlogy, 2004; pp 352-356.

53. Chang, Z.; Yan, W.; Shang, J., *et al.*, Piezoelectric properties of graphene oxide: A first-principles computational study. *Applied Physics Letters* **2014,** *105* (2).

54. Yang, J.; Zhang, Y.; Li, Y., *et al.*, Piezoelectric Nanogenerators based on Graphene Oxide/PVDF Electrospun Nanofiber with Enhanced Performances by In-Situ Reduction. *Materials Today Communications* **2021,** *26*, 101629.

55. Alamusi; Xue, J.; Wu, L., *et al.*, Evaluation of piezoelectric property of reduced graphene oxide (rGO)–poly(vinylidene fluoride) nanocomposites. *Nanoscale* **2012,** *4* (22), 7250-7255.

56. Williamson, B. J.; Pastiroff, S.; Cressey, G., Piezoelectric properties of quartz and cristobalite airborne particulates as a cause of adverse health effects. *Atmospheric Environment* **2001,** *35* (20), 3539-3542.

57. Zhu, Q.; Song, X.; Chen, X., *et al.*, A high performance nanocellulose-PVDF based piezoelectric nanogenerator based on the highly active CNF@ZnO via electrospinning technology. *Nano Energy* **2024,** *127*, 109741.

58. Vadhel, K. V.; Joshi, J. H.; Kochuparampil, A. P., *et al.*, The influence of l-ornithine monohydrochloride on growth and various properties of ammonium dihydrogen phosphate crystals. *Optical Materials* **2022,** *134*, 113136.

59. Rajesh, P.; Ramasamy, P.; Kumar, B., *et al.*, Effect of cobalt and dl-malic acid on the growth rate, crystalline perfection, optical, mechanical, dielectric, piezoelectric properties and SHG efficiency of ADP single crystals. *Physica B: Condensed Matter* **2010,** *405* (10), 2401-2406.

60. Prasad, B. B.; Pandey, I., Molecularly imprinted polymer-based piezoelectric sensor for enantio-selective analysis of malic acid isomers. *Sensors and Actuators B: Chemical* **2013,** *181*, 596-604.

61. Lemaire, E.; Thuau, D.; De Vaulx, J. B., *et al.*, Rochelle Salt-Based Ferroelectric and Piezoelectric Composite Produced with Simple Additive Manufacturing Techniques. *Materials (Basel)* **2021,** *14* (20).

62. Manzor, B.; Daly, J. H.; Islam, M. S., *et al.*, Ultrasonic and dielectric investigation of N-methylurea. *Journal of the Chemical Society, Faraday Transactions* **1997,** *93* (21), 3799-3805.

63. An, L.-C.; Zhao, C.; Zhao, Y., *et al.*, Chiral 1D Hybrid Metal Halides with Piezoelectric Energy Harvesting and Sensing Properties. *Small Structures* **2023,** *4* (11), 2300135.

64. Sukhanov, G. T.; Bosov, K. K.; Filippova, Y. V., *et al.*, New 5-Aminotetrazole-Based Energetic Polymers: Synthesis, Structure and Properties. *Materials* **2022,** *15* (19), 6936.

65. Bhukkal, S.; Kumar, B., Electrical, optical, and mechanical properties of modified Czochralski grown organic 4-nitrobenzaldehyde single crystal. *Journal of Physics and Chemistry of Solids* **2022,** *169*, 110839.

66. Bento, A. P.; Hersey, A.; Félix, E., *et al.*, An open source chemical structure curation pipeline using RDKit. *Journal of Cheminformatics* **2020,** *12* (1), 51.

67. O'Boyle, N. M.; Banck, M.; James, C. A., *et al.*, Open Babel: An open chemical toolbox. *J Cheminform* **2011,** *3*, 33.